



Published in final edited form as:

*J Biomol NMR*. 2015 April ; 61(0): 249–260. doi:10.1007/s10858-014-9883-6.

## Structure Refinement and Membrane Positioning of Selectively Labeled OmpX in Phospholipid Nanodiscs

Franz Hagn<sup>1,2</sup> and Gerhard Wagner<sup>1</sup>

<sup>1</sup>Dept. of Biological Chemistry and Molecular Pharmacology, Harvard Medical School, Boston, MA 02115, USA

<sup>2</sup>Dept. of Chemistry and Institute for Advanced Study, Technische Universität München, 85748 Garching, Germany

### Abstract

NMR structural studies on membrane proteins are often complicated by their large size, taking into account the contribution of the membrane mimetic. Therefore, classical resonance assignment approaches often fail. The large size of phospholipid nanodiscs, a detergent-free phospholipid bilayer mimetic, prevented their use in high-resolution solution-state NMR spectroscopy so far. We recently introduced smaller nanodiscs that are suitable for NMR structure determination. However, side-chain assignments of a membrane protein in nanodiscs still remain elusive. Here, we utilized a NOE-based approach to assign (stereo-) specifically labeled Ile, Leu, Val and Ala methyl labeled and uniformly <sup>15</sup>N-Phe and <sup>15</sup>N-Tyr labeled OmpX and calculated a refined high-resolution structure. In addition, we were able to obtain residual dipolar couplings (RDCs) of OmpX in nanodiscs using Pf1 phage medium for the induction of weak alignment. Back-calculated NOESY spectra of the obtained NMR structures were compared to experimental NOESYs in order to validate the quality of these structures. We further used NOE information between protonated lipid head groups and side-chain methyls to determine the position of OmpX in the phospholipid bilayer. These data were verified by paramagnetic relaxation enhancement (PRE) experiments obtained with Gd<sup>3+</sup>-modified lipids. Taken together, this study emphasizes the need for the (stereo-) specific labeling of membrane proteins in a highly deuterated background for high-resolution structure determination, particularly in large membrane mimicking systems like phospholipid nanodiscs. Structure validation by NOESY back-calculation will be helpful for the structure determination and validation of membrane proteins where NOE assignment is often difficult. The use of protein to lipid NOEs will be beneficial for the positioning of a membrane protein in the lipid bilayer without the need for preparing multiple protein samples.

### Keywords

NOESY back-calculation; membrane proteins; non-uniform sampling; RDCs; selective labeling; structure

## Introduction

Membrane proteins are involved in many biological processes ranging from signal transduction to the exchange of metabolites across biological membranes. Therefore, this protein class is of high interest for many biological problems and particularly drug design applications. In order to facilitate drug design, a structure-based approach is considered most effective. Unfortunately, compared to the plethora of structural data on soluble proteins much less is known about structures of integral membrane proteins. This is primarily due to difficulties of producing integral membrane proteins in folded and active forms as well as in sufficient yields. A major part of this problem is the selection of an appropriate membrane-mimicking environment supporting both function and stability of a particular membrane protein. Usually detergents are employed for membrane protein preparation and detergent micelles are the most common media for structural investigations. However, crystal structures of membrane proteins solubilized in detergents often contain bound lipids emphasizing the beneficial effect of a lipid environment for their structure and stability. In many cases, the use of a detergent-free environment is required for the study of biological interactions, where membrane proteins interact with other membrane proteins or soluble proteins. There, detergents used for the solubilization of individual membrane proteins are often not compatible and soluble proteins might precipitate in presence of detergents. The use of phospholipid bilayers can overcome these problems, as they resemble a considerably more native membrane environment that does not destabilize soluble proteins.

The recent introduction of phospholipid nanodiscs (Denisov et al. 2004; Nath et al. 2007) as membrane mimetic appears promising for studying membrane proteins in phospholipid bilayers by solution NMR. The formation of nanodiscs is based on the observation that apolipoprotein A-I (Apo A-I) can wrap around small patches of bilayer creating small membrane-like, disc-shaped particles of defined size (Fang et al. 2003; Krieger et al. 1978). Different versions of Apo A-I have been engineered for biophysical studies and are called membrane-scaffolding proteins (MSPs). This system has the potential to be a widely used membrane mimetic with the advantage of closely resembling a native-like lipid environment.

To this end, nanodiscs are the only available detergent-free membrane mimetic for solution NMR spectroscopy and are in addition suitable for studying protein-protein interactions in an unbiased lipid bilayer environment. It is therefore highly desirable to be able to structurally characterize membrane proteins in this promising system by NMR. The shortest commonly used version of the MSP constructs produces discs of around 10 nm in diameter, which translates into a molecular weight of 150–200 kDa. These nanodiscs were already successfully used for the incorporation of membrane proteins like VDAC-1 (Raschle et al. 2009) and -2 (Yu et al. 2012), CD4mut (Gluck et al. 2009) and the voltage-sensing domain of the potassium channel KvAP (Shenkarev et al. 2010) for 2D-heteronuclear NMR experiments. More recently, a partial assignment of OmpA in nanodiscs was reported (Susac et al. 2014). However, the use of nanodiscs for multidimensional NMR experiments as required for structure determination had remained elusive due to the still large molecular weight of these particles. In order to overcome this obstacle we recently introduced a series

of truncated MSPs that form subsequently smaller nanodiscs that are suitable for the high-resolution structure determination of membrane proteins (Hagn et al. 2013).

Structure determination of large proteins and in particular membrane proteins is a challenging task, due to a high degree of signal overlap and line broadening caused by slow tumbling. In order to improve the relaxation properties of large proteins, protein deuteration is commonly used to reduce relaxation induced by dipolar interactions. However, in order to determine protein structures, especially of  $\alpha$ -helical proteins, side-chain contacts are required. This problem has been alleviated by the introduction of protonated methyl probes into leucine, valine and isoleucine (Goto et al. 1999; Tugarinov et al. 2006) or alanine (Ayala et al. 2009) side chains and further refined by the use of stereospecific leucine/valine methyl labeling (Gans et al. 2010). These approaches drastically extended the size limit for NMR structure determination and facilitated, e.g. the structure determination of the 82kDa protein malate synthase (Tugarinov et al. 2005).

Here, we set out to include side-chain information for NMR-based structure determination of a membrane protein in our optimized MSP1D1 H5 nanodisc. In order to facilitate the assignment of side chain methyl groups of OmpX, we produced stereospecifically Ile, Leu, Val methyl-labeled and  $^{13}\text{C}$  Ala methyl labeled protein in a highly deuterated background. In addition, we incorporated  $^{15}\text{N}$ -labeled Phe and Tyr into the protein, which provided NOE information on their side-chain conformation. Using this approach, we were able to assign all labeled side-chain methyl and most of the aromatic resonances. The obtained high-resolution structural bundle of OmpX in phospholipid nanodiscs showed a very low r.m.s.d. for the ordered regions and, compared to the crystal structure of OmpX, very similar but not completely identical side-chain orientations are observed for the transmembrane  $\beta$ -barrel. The extra-membrane part of the NMR structure is dynamic and does not show any ordered secondary structure. The obtained structures were used for NOESY back-calculation and the resulting spectra were compared to the experimental data in order to validate the quality of these structures. Finally, we used NOE information between protonated lipid head groups and OmpX side-chain methyls and backbone amides as well as paramagnetic relaxation enhancements using  $\text{Gd}^{3+}$ -modified lipids to position the protein within the lipid bilayer. Following this protocol, the high-resolution structure determination and positioning of membrane proteins in a phospholipid bilayer can be achieved in an efficient manner, thus further streamlining the time-consuming process of membrane protein structure determination.

## Results

### Stereospecific labeling of OmpX

In order to obtain a sufficiently high proton density in OmpX for NOESY experiments in a highly deuterated background, we added the stereospecific Leu/Val precursor ethyl 2-hydroxy 2- $^{13}\text{C}$ -methyl 3-oxobutanoate (Gans et al. 2010; Plevin et al. 2011) together with  $\alpha$ -ketobutyrate (Goto et al. 1999) to achieve Ile- $\delta$  labeling, according to established protocols, and the amino acids  $^{15}\text{N}$ -Phe and  $^{15}\text{N}$ -Tyr as well as 3- $^{13}\text{CH}_3$ -2-D-Ala together with deuterated succinate (Ayala et al. 2009) to M9 medium in 99%  $\text{D}_2\text{O}$  and  $^2\text{H}$ ,  $^{12}\text{C}$  Glucose and  $^{15}\text{NH}_4\text{Cl}$ . This setup yielded  $^2\text{H}$ ,  $^{15}\text{N}$  OmpX  $^{13}\text{CH}_3$ -labeled at Ile- $\delta$ , Val- $\gamma_2$ , Leu- $\delta_2$  and

Ala- $\beta$  and uniformly  $^{15}\text{N}$ ,  $^1\text{H}$ -labeled Phe and Tyr. The amount of protons introduced into the protein provided a dense proton network for NOE-based methyl group assignment and a subsequent high-resolution structure determination (Fig. 1A). We incorporated OmpX into nanodiscs composed of our MSP1D1 H5 (Hagn et al. 2013) and deuterated DMPC/DMPG lipids (Fig. 1B), which yielded a particle of 8nm in diameter (Fig. 1C) and a correlation time of 34ns (see (Hagn et al. 2013)).

### NOE-based resonance assignment

For the assignment of methyl group resonances, we employed a NOE-based approach. Due to the low methyl group density and based on our previous backbone assignment (Fig. 2A) and the previously solved structure of OmpX, we were able to assign all signals in the 2D- $^{13}\text{C}$ ,  $^1\text{H}$ -HMQC (Fig. 2B). In order to obtain reliable NOE assignments, we recorded a suite of four 3D-NOESY experiments: 3D- $^{13}\text{C}$ -edited- $^1\text{H}$ - $^1\text{H}$ -NOESY, 3D- $^{15}\text{N}$ -edited- $^1\text{H}$ - $^1\text{H}$ -NOESY, 3D- $^{13}\text{C}$ ,  $^{13}\text{C}$ -edited- $^1\text{H}$ - $^1\text{H}$ -NOESY, 3D- $^{13}\text{C}$ ,  $^{15}\text{N}$ -edited- $^1\text{H}$ - $^1\text{H}$ -NOESY, where the chemical shifts of the proton-connected heteronuclei could be obtained. For each of the amino acid residues containing  $^{13}\text{C}$ ,  $^1\text{H}$ -labeled methyl-groups, a specific assignment approach had to be adapted (Fig. 2C–E). For Alanine, which was not  $^{15}\text{N}$  labeled, the methyl group assignment had to be obtained by using an NOE contact from the succeeding amide to the alanine methyl group and vice versa, together with long-range NOE contacts arising from the tertiary structure (Fig. 2C, left panel). For longer side chains bearing methyl groups, like Isoleucine and Leucine, an NOE contact between the assigned amide nitrogen/proton pair and the terminal  $\delta$  methyl group cannot be observed in all cases. Therefore, the methyl group assignment has to be established by considering the tertiary structure. In the case of the Ile40  $\delta$ 1 methyl group, no NOE could be observed to its own amide group in the 3D- $^{15}\text{N}$ -edited- $^1\text{H}$ ,  $^1\text{H}$ -NOESY experiment (Fig. 2C, center left panel). However, looking from the methyl group in an 3D- $^{13}\text{C}$ -edited- $^1\text{H}$ ,  $^1\text{H}$ -NOESY experiment, a weak NOESY signal to its amide showed up, as well as a characteristic NOESY pattern to methyls, aromatics and amide groups in close proximity. With a good initial structural model at hand, which was calculated based on backbone amide contacts only, this pattern can then be used to unambiguously assign the methyl group. A similar but slightly more straightforward situation is present for the Leu113  $\delta$ 2 methyl (Fig. 2C–E, center right panel). Here, the 3D- $^{15}\text{N}$ -edited- $^1\text{H}$ ,  $^1\text{H}$ -NOESY experiment shows a clear contact from the amide to the intra-residue methyl group. Again, the characteristic pattern of NOE contacts in combination with a structural model facilitated the assignment of the methyl group with high confidence. For Valine residues, there is usually a strong intra-residual NOE contact between the amide and the methyl group, as shown in the case of Val83  $\gamma$ 2 methyl (Fig. 2C–E, right panel). In addition to the clear inter-residual contact, the network of connectivities again leads to an unambiguous assignment of the methyl resonance. The presence of protonated Phe and Tyr residues in the protein is very helpful for the establishment of a dense NOE network. In general, the assignment of these residues can be achieved with a 3D- $^{15}\text{N}$ -edited- $^1\text{H}$ ,  $^1\text{H}$ -NOESY experiment. The assignments of ILV methyl groups were similar to those previously obtained for OmpX in DHPC micelles (Hilty et al. 2002; Hilty et al. 2003). However, we here additionally labeled and assigned Alanine methyl groups, and Phe and Tyr aromatic resonances to increase proton density for structure determination.

## Side-chain and residual dipolar coupling (RDC) based structural refinement of OmpX in nanodiscs

The protocol for methyl group assignment described in the previous section simultaneously provided distance information for the high-resolution structure determination of OmpX. We collected a large number of methyl-to-amide, methyl-to-methyl, methyl-to-aromatic and amide-to-aromatic NOEs as shown in table 1. Due to a still low proton density in the protein and a rather long NOESY mixing time of 300ms, we were able to observe distances of up to 7–8Å. For ordered  $\beta$ -barrel regions, as defined in table 1, the resulting structure shows an r.m.s.d. of 0.2 Å and 0.9 Å for backbone and non-hydrogen atoms, respectively (Fig. 3A, Table 1). The orientation of all side-chains, where NOE information could be collected, was well defined. Side-chains pointing inward of the  $\beta$ -barrel of OmpX showed excellent clustering, whereas side-chains pointing toward the membrane were generally less well defined, especially amino acids within the flexible loop regions. This refined structure of OmpX overlays very well with the  $\beta$ -barrel part of the X-ray structure (Vogt and Schulz 1999) (1QJ8.pdb) obtained earlier (Fig. 3B). The distal part of the  $\beta$ -barrel is approximately 10 Å wide, whereas this part of the structure showed a larger diameter of 15 Å in our recent NMR structure that is based on backbone amide-to-amide NOEs only (Hagn et al. 2013) (Fig. 3B). This difference is most likely due to the lack of side-chain-to-side-chain NOEs, which leads to a tighter packing of side-chains in the terminal parts of the  $\beta$ -barrel. In line with our previous structure, we here also observe mainly unstructured external loops of OmpX, in contrast to the X-ray structure.

We next investigated the possibility of obtaining residual dipolar couplings of OmpX in nanodiscs using conventional Pf1-phage medium for alignment, as previously described by others (Bibow et al. 2014). We here used a Pf1 concentration of 10mg/ml, which yielded an HDO quadrupolar splitting of 8.8Hz at a magnetic field strength of 900MHz proton frequency and at a temperature of 40°C (Fig. 3C). We also tested the use of Pf1-phages for the weak alignment of OmpX in DPC micelles (100mM DPC) but could not observe any HDO splitting, most likely due to the denaturing effect of DPC on the Pf1-phage structure. Problems of aligning membrane proteins in micelles using Pf1-phage have been reported previously and other alignment methods have been used (Bellot et al. 2013; Douglas et al. 2007). For the nanodisc system, we obtained 70 H-N RDCs and used these data for an RDC-based structural refinement of the NOE-based structure. The correlation of experimental and back-calculated RDCs, using the RDC-refined structure, was very good ( $Q=0.12$ ,  $R=0.94$ ) and the deviations were within the error of the experiment ( $RMS=1.4Hz$ ). The RDC-refined and the NOE-structure of OmpX showed an almost identical secondary structure content and orientation of  $\beta$ -strands. This emphasizes the practical value of RDCs for structure validation and refinement, and the benefit of nanodiscs for using convenient alignment media for obtaining membrane protein RDCs.

## NOESY back-calculation as a tool for structure validation and refinement of membrane proteins

We next set out to validate the structures obtained with NMR and to compare those structures with the crystal structure (pdb code: 1qj8). An overlay of the three structures in figure 4C shows a low mutual backbone r.m.s.d., but there are apparent differences in the

orientation of side-chains. As a measure of the side-chain orientation we extracted  $\chi_1$  angles of all three structures using the program Procheck-NMR (Laskowski et al. 1996) and plotted these values against the residue number of OmpX (Fig. 4A). All structures populate  $\chi_1$  angles of around  $-60^\circ$  ( $g^+$ ),  $+60^\circ$  ( $g^-$ ) or  $180^\circ$  (trans), within an approximate error of  $\pm 30^\circ$ . The degree of correlation of these angles between the NMR and the crystal structure was further analyzed by comparing the number of  $\chi_1$  angles that are identical to those in the crystal structure. For all residues in OmpX the agreement is higher for the experimental structure based on backbone and side-chain NMR data than for the structure based on backbone constraints only (49 vs. 40%, Fig. 4B). These numbers are of course biased by differences in secondary structure between the NMR and crystal structures. In addition, due to the fact that outside facing, i.e. toward the lipid bilayer, residues are less restricted in their side-chain conformation than residues that are more tightly packed in the interior, we performed the same type of analysis with residues that are oriented toward the interior of the  $\beta$ -barrel. There, the overlap between NMR side-chain and X-ray structure remains about the same (44%), indicating that all side-chains are already well defined in the side-chain based NMR structure. The NMR backbone structure performs surprisingly well in that comparison with 55% of all inside-facing side-chains showing a  $\chi_1$  angle identical to the crystal structure. The absence of any side-chain contact information in the backbone NMR structure and the very good performance compared to the crystal structure argues for the beneficial influence of state-of-the-art force fields used for NMR structure calculations (MacKerell 2001). The outside-facing side chains are not restricted by packing and are consequently less well defined in the backbone structure, as indicated by a higher heavy atom r.m.s.d. of  $1.3 \text{ \AA}$  (Hagn et al. 2013) vs.  $0.9 \text{ \AA}$  for the refined NMR structure. In the  $\beta$ -barrel interior, there is a higher degree of side-chain packing and thus a lower degree of freedom, which apparently is enough to restrict the side chain orientation, especially for a relatively small  $\beta$ -barrel protein.

However, these results also argue for the need of a more thorough evaluation procedure of the OmpX structure in solution, without the requirement of a reference structure. The crystal structure used here introduces errors to the analysis due to the inherent flexibility of side chains and effects caused by crystal packing, which are absent in solution.

Therefore, we decided to perform an additional structure validation step and further assess the quality of these structures by NOESY back-calculation. For NOESY back-calculation the program NMRspiritC++ (Murray Coles, personal communication, see methods section) was used. We compared the experimental and back-calculated NOESY spectra in each case, i.e. for the NMR side-chain, NMR backbone and X-ray structures (Fig. 4D). As can be seen for Leucine 26 methyl  $\delta_2$ , there are differences in the back-calculated NOE connectivity patterns. The comparison with the experimental NOESY strip reveals that the NMR, but also the X-ray structure, shows good fit. They both exhibit a  $\chi_1$  angle of  $-60^\circ$ , whereas in the NMR backbone structure, this angle is  $180^\circ$ . In this case an angle of  $-60^\circ$  is most likely correct. The absence of an NOE to another methyl group ( $\sim 1.3 \text{ ppm}$ , Val5  $\gamma_2$ ) in the back-calculated NOESY using the crystal structure may be due to slight difference of the exact rotamer and a resulting change in distance. In the case of Valine 39 methyl  $\gamma_2$ , the NMR side-chain and backbone structures seem to be more consistent with the experimental data than the X-ray structure, with the side-chain refined structure again showing the best fit. The NOE contact to Ala67- $\beta$  ( $\sim 1.35 \text{ ppm}$ ) is only present in both NMR structures. As Val39 is

facing toward the lipid bilayer, deviations in the crystal structure might therefore be induced by crystal contacts that are not present in solution. Finally, for Leucine 123 methyl  $\delta 2$ , all three back-calculated NOESY spectra show a very good agreement with the experimental NOESY. A NOESY contact to Ala142- $\beta$  (~1.6ppm) shows up only in the refined NMR but is missing in the other two structures, even though all structures adopt the same  $\chi 1$  angle. However, due a different  $\chi 2$  angle in the NMR backbone structure, this NOE contact is not present there. In the crystal structure, the distance between both methyl groups is too far to give rise for a back-calculated NOE cross peak. Additional resonances in the experimental NOESY are due to missing assignments that are not considered for back-calculation or NOE contacts between the protein and the lipids, which show some degree of residual protonation (indicated by red asterisks and lines in Fig. 4D).

Overall, the method of structure validation by NOESY back-calculation seems to be a suitable tool for membrane proteins, where a full characterization of side-chain orientations might not be possible in many cases. This strategy should improve the quality of membrane protein structures. Unfortunately, so far this requires a significant amount of manual interference, and it is therefore desirable to develop software tools that combine structure calculation and reliable NOESY back-calculation, as well as structural editing in the future.

### OmpX membrane position based on protein-to-lipid NOEs

Along with accurate structure determination of membrane proteins, the correct positioning of the protein in the membrane is of utmost importance for assessing its biological function and its exposed surface area available for interaction with partner proteins and small molecules. Therefore, we here used two approaches to gather information on the position of OmpX in a phospholipid bilayer membrane, mimicked by nanodiscs. First, we used NOESY spectra of selectively ILVA and F/Y labeled OmpX in MSP1D1 H5 nanodiscs formed with deuterated DMPC/PG lipids. Due to residual protonation of the fatty acids in the lipids and the presence of protonated lipid head groups, we were able to observe NOEs from OmpX to various regions in the lipid (Fig. 5A). There is a clear correlation between the position of a particular backbone amide or side-chain methyl group and the observed NOE signals, which allows for the positioning of the protein within the lipid bilayer. For side chains facing toward the phospholipid bilayer, like Ala142, strong NOE signals between the alanine methyl group and the aliphatic chains of the lipids can be observed. Inward-facing side-chains like Ile40 show no or markedly reduced NOEs to the lipid. Residues located close to or at the lipid head group region of the phospholipid bilayer exhibit weak or strong NOEs to the glycerol and choline moieties of the lipid, respectively, as shown in Fig. 5A for L113 and V39. There are computational tool for the prediction of the membrane position, e.g. the PPM server (Lomize et al. 2006). For OmpX, this tool provides a slightly tilted membrane position, as shown in figure 5B. In order to validate this result, we quantified the intensity of NOE signals from all backbone amides of OmpX to the aliphatic and head group regions of the lipids (Fig. 5C). The results show that the aliphatic chains of the lipids exhibit strong NOEs to the regions in OmpX embedded in the phospholipid bilayer, whereas regions located outside of the bilayer show strong NOEs to the lipid head group region, as indicated by the red color in figure 5C. The pattern of the detected NOE intensities suggests a similar tilt angle as predicted by the PPM server.

We furthermore employed paramagnetic relaxation enhancement for membrane protein positioning. Due to the possibility to use any blend of lipids for nanodisc assembly, we added the paramagnetic lipid Gd-DTPA-DMPE (Bertini et al. 2004) (Fig. 5D), where a paramagnetic gadolinium ion is complexed by a DTPA group attached to the ethanolamine of the DMPE lipid, to our nanodisc preparations. This paramagnetic agent has been successfully applied to determine the position of membrane-tethered Rheb1 relative to the phospholipid bilayer membrane (Mazhab-Jafari et al. 2013). We then compared the signal intensities in 2D- $^{15}\text{N}$ , $^1\text{H}$ -TROSY experiments of  $^2\text{H}$ ,  $^{15}\text{N}$ -labeled OmpX in paramagnetic and DMPC/PC-only nanodiscs, respectively. The obtained relative intensity pattern (Fig. 5D) reflects the position of OmpX in the phospholipid bilayer. Low bars indicate regions close to head group region or outside of the bilayer, whereas high relative intensity reflects protection by the phospholipid bilayer, i.e. the respective residue is located in the bilayer. Color-coding of these data on the OmpX structure provides a similar picture as obtained by NOE information. Part of the  $\beta$ -barrel is located outside the hydrophobic region of the bilayer, whereas the bottom part of OmpX, except loop regions between the  $\beta$ -strands, sits in the bilayer.

## Discussion

NMR experiments on membrane proteins are still a challenge due to their large size, the high degree of spectral overlap and problems in finding appropriate membrane mimics that sufficiently stabilize the protein for structural studies. We here showed that we can 1.) Use smaller phospholipid bilayer nanodiscs to cut down the size of the membrane mimic as much as possible, 2.) Perform (stereo-) selective amino acid labeling of Ala, Ile, Leu and Val residues to reduce the spectral complexity, especially in carbon-edited and NOESY experiments, 3.) Use phospholipid nanodiscs as a membrane mimetic, providing a native environment that confers high long-term stability to the membrane protein of interest and facilitates the study of membrane proteins in a real, detergent-free planar phospholipid bilayer membrane, 4.) Use NOESY back-calculation to validate NMR structural models by comparing back-calculated to the experimental spectra, and finally 5.) Define the position of the membrane protein of interest by protein-to-lipid NOE or PRE data. Due to the incorporation of side-chain information and the possibility for in depth structure validation this protocol facilitates the accurate high-resolution structure determination of membrane proteins.

In general, this protocol works well with  $\beta$ -barrel proteins where a decent structural model can be obtained using backbone NOEs only. For  $\alpha$ -helical proteins, whose structure determination requires side chain contacts, this task becomes a bit more complicated. In case of the availability of homologous structures in the protein data bank, a decent starting model may be generated by homology modeling. However, for *de novo* structure determination a starting structure needs to be obtained by site directed spin labeling (Altenbach et al. 1990) and subsequent paramagnetic relaxation experiments (Battiste and Wagner 2000). Once a roughly correct tertiary fold is obtained, iterative cycles of NOE peak assignment and NOESY back-calculation will provide a subsequent refinement of the initial model. The use of chemical shifts, NOE and PRE information for *de novo* methyl group assignment has been recently implemented in other software packages (Chao et al. 2012; Venditti et al.



2011; Xu et al. 2009). It will be therefore beneficial to include these approaches into our resonance assignment and structure calculation protocol to speed up the time-consuming assignment process.

In comparison to combined automated NMR NOE assignment and structure calculation approaches (Herrmann et al. 2002; Linge et al. 2003) this workflow involves a significant amount of manual interference, thus resolving problems arising from signal overlap and missing resonances, which are common issues with membrane proteins. However, for making this approach more efficient, NOESY back-calculation needs to be integrated into structure visualization and editing software in order to obtain on-the-fly spectra once a side-chain rotamer is manually altered. This approach, possibly in combination with automated assignment methods mentioned above, may turn out to be helpful for the structure determination of challenging membrane proteins, where NMR resonance assignment is difficult, and it may be a quick way of detecting structural changes happening upon ligand or partner protein binding.

Back-calculation of 3D NOESY spectra from the calculated spectra has been used here to validate the structural models. It showed that most but not all side-chain conformations agree between the NMR and X-ray structures for the defined part of the membrane protein. Ultimately, a refinement minimizing the difference between calculated and experimental spectra would be desirable. However, this will require a major effort.

## Methods

### Protein expression and purification

Production of OmpX and MSPD1 H5 protein was done as previously described (Hagn et al. 2013). For selective labeling of OmpX, *E. coli* BL21(DE3) cells transformed with pET11a-OmpX were grown in M9 media in 99% D<sub>2</sub>O (Isotech) supplemented with 2g/L <sup>2</sup>H, <sup>12</sup>C-Glucose (Isotech) and 1g/L <sup>15</sup>NH<sub>4</sub>Cl. 300mg/L stereospecific LV precursor ethyl 2-hydroxy 2-<sup>13</sup>C-methyl 3-oxobutanoate (according to protocols by the Boisbouvier lab (Gans et al. 2010; Plevin et al. 2011)) and 80mg/L of the Ile precursor  $\alpha$ -ketobutyrate (Goto et al. 1999) together with 2.5g/L d<sub>4</sub>-succinate (CIL) and 0.8g/L 3-[<sup>13</sup>CH<sub>3</sub>]-2-D-Ala (CIL), as well as 80mg/L U-[<sup>15</sup>N]-Phe and Tyr (CIL) were added to the bacterial culture approximately 1h before induction with 1mM IPTG. The choice of the Leu/Val precursor resulted in <sup>13</sup>CH<sub>3</sub> labeling of the *pro-S* methyl group in both amino acids in an otherwise per-deuterated <sup>12</sup>C background. The culture was shaken at 37°C for 8 more hours and harvested, refolded and purified as described previously (Hagn et al. 2013).

### Nanodisc assembly

Nanodisc formation was done in a volume of 3mL (200 $\mu$ M OmpX in DPC, 400 $\mu$ M MSPD1 H5, 13mM DMPC:DMPG=3:1). The mixture was incubated at RT for 2h and subsequently the detergent was removed by the addition of 2g Biobeads-SM2 (Biorad) and gentle shaking at RT for >4h. Assembled nanodiscs were further purified on a S200 size exclusion column (125mL bed volume). A symmetric peak at V<sub>e</sub>~80mL was collected and concentrated to 1mM using Amicon (Millipore) centrifugal devices (30kDa MWCO). For

NMR experiments 5% (v/v) D<sub>2</sub>O were added to the sample for frequency and lock stabilization. Nanodisc doped with the paramagnetic agent Gd-DTPA-DMPE (Avanti Polar Lipids) were prepared in the same manner except that the Gd<sup>3+</sup>-compound was added in a ratio of 1:20 (2 molecules per membrane leaflet).

### NMR spectroscopy and structure calculation

NMR experiments were done on Bruker AvanceIII spectrometers operating at 800MHz and 900MHz proton frequency with a cryogenic probe and using Topspin 3.2. All 3D experiments were run in a non-uniformly sampled (NUS) manner with 15–20% sampling density and an NOE mixing time of 300ms and at 318K. NUS setup was facilitated by our recently published NUS schedule generator (Hyberts et al. 2012) that utilizes Poisson-gap sampling (Hyberts et al. 2010). For rapid spectra reconstruction we employed iterative soft thresholding (IST) (Hyberts et al. 2012). All 3D spectra were processed with NMRpipe (Delaglio et al. 1995). All other spectra were processed with Topspin3.2 (Bruker Biospin). Data analysis was done with Sparky (Goddard and Kneller, UCSF) and structure calculation was performed with Xplor-NIH (Schwieters et al. 2003) using standard protocols. For RDC analysis the program Pales (Zweckstetter 2008) was used.

### NOESY back-calculation

For NOESY back-calculation we used an in-house version of the previously published program SPIRIT (Zhu et al. 1998), called NMRSpiritC++ (Murray Coles, MPI Tübingen, personal communication). This extended version of the program is capable of the back-calculation of various 3D-NOESY spectra involving one or two heteronuclear dimensions (e.g. HCH-NOESY, HNH-HOESY, CCH-NOESY, CNH-NOESY)(Diercks et al. 1999). A correlation time of 34ns and NOE mixing time of 300ms was used; all other parameters were identical to the experimental setup. Calculated spectra were displayed with Sparky and compared to the experimental data. Requests for obtaining the NMRSpiritC++ software may be addressed to Dr. Murray Coles (murray.coles@tuebingen.mpg.de).

### Acknowledgements

This work was supported by a Human Frontier Science Program (HFSP) long-term and a TUM-IAS Hans-Fischer fellowship (to F.H.). G.W. acknowledges support from NIH through grants GM075879, GM047467, GM094608 and EB002026. F.H. acknowledges the support of the Technische Universität München – Institute for Advanced Study, funded by the German Excellence Initiative and the European Union Seventh Framework Program under grant agreement n° 291763. We thank Dr. Murray Coles (MPI Tübingen, Germany) for providing NMRSpiritC++ software, Dr. Sven Hyberts (Harvard Medical School) for help with NMR non-uniform sampling setup and Dr. Vlado Gelev (FB reagents, Cambridge, MA) for the custom synthesis of deuterated lipids and isotope precursors.

### References

- Altenbach C, Marti T, Khorana HG, Hubbell WL. Transmembrane protein structure: spin labeling of bacteriorhodopsin mutants. *Science*. 1990; 248:1088–1092. [PubMed: 2160734]
- Ayala I, Sounier R, Use N, Gans P, Boisbouvier J. An efficient protocol for the complete incorporation of methyl-protonated alanine in perdeuterated protein. *J Biomol NMR*. 2009; 43:111–119. [PubMed: 19115043]
- Battiste JL, Wagner G. Utilization of site-directed spin labeling and high-resolution heteronuclear nuclear magnetic resonance for global fold determination of large proteins with limited nuclear overhauser effect data. *Biochemistry*. 2000; 39:5355–5365. [PubMed: 10820006]

- Bellot G, McClintock MA, Chou JJ, Shih WM. DNA nanotubes for NMR structure determination of membrane proteins. *Nat Protoc.* 2013; 8:755–770. [PubMed: 23518667]
- Bertini I, et al. Persistent contrast enhancement by sterically stabilized paramagnetic liposomes in murine melanoma. *Magnetic resonance in medicine : official journal of the Society of Magnetic Resonance in Medicine / Society of Magnetic Resonance in Medicine.* 2004; 52:669–672.
- Bibow S, Carneiro MG, Sabo TM, Schwiegl C, Becker S, Riek R, Lee D. Measuring membrane protein bond orientations in nanodiscs via residual dipolar couplings. *Protein science : a publication of the Protein Society.* 2014; 23:851–856. [PubMed: 24752984]
- Chao FA, Shi L, Masterson LR, Veglia G. FLAMEnGO: a fuzzy logic approach for methyl group assignment using NOESY and paramagnetic relaxation enhancement data. *J Magn Reson.* 2012; 214:103–110. [PubMed: 22134225]
- Delaglio F, Grzesiek S, Vuister GW, Zhu G, Pfeifer J, Bax A. NMRPipe: a multidimensional spectral processing system based on UNIX pipes. *J Biomol NMR.* 1995; 6:277–293. [PubMed: 8520220]
- Denisov IG, Grinkova YV, Lazarides AA, Sligar SG. Directed self-assembly of monodisperse phospholipid bilayer Nanodiscs with controlled size. *J Am Chem Soc.* 2004; 126:3477–3487. [PubMed: 15025475]
- Diercks T, Coles M, Kessler H. An efficient strategy for assignment of cross-peaks in 3D heteronuclear NOESY experiments. *J Biomol NMR.* 1999; 15:177–180. [PubMed: 20872110]
- Douglas SM, Chou JJ, Shih WM. DNA-nanotube-induced alignment of membrane proteins for NMR structure determination. *Proc Natl Acad Sci U S A.* 2007; 104:6644–6648. [PubMed: 17404217]
- Fang Y, Gursky O, Atkinson D. Lipid-binding studies of human apolipoprotein A-I and its terminally truncated mutants. *Biochemistry.* 2003; 42:13260–13268. [PubMed: 14609337]
- Gans P, et al. Stereospecific isotopic labeling of methyl groups for NMR spectroscopic studies of high-molecular-weight proteins. *Angewandte Chemie.* 2010; 49:1958–1962. [PubMed: 20157899]
- Gluck JM, Wittlich M, Feuerstein S, Hoffmann S, Willbold D, Koenig BW. Integral membrane proteins in nanodiscs can be studied by solution NMR spectroscopy. *J Am Chem Soc.* 2009; 131:12060–12061. [PubMed: 19663495]
- Goto NK, Gardner KH, Mueller GA, Willis RC, Kay LE. A robust and cost-effective method for the production of Val, Leu, Ile ( $\delta$  1) methyl-protonated  $^{15}\text{N}$ -,  $^{13}\text{C}$ -,  $^2\text{H}$ -labeled proteins. *J Biomol NMR.* 1999; 13:369–374. [PubMed: 10383198]
- Hagn F, Etkorn M, Raschle T, Wagner G. Optimized phospholipid bilayer nanodiscs facilitate high-resolution structure determination of membrane proteins. *J Am Chem Soc.* 2013; 135:1919–1925. [PubMed: 23294159]
- Herrmann T, Guntert P, Wuthrich K. Protein NMR structure determination with automated NOE assignment using the new software CANDID and the torsion angle dynamics algorithm DYANA. *J Mol Biol.* 2002; 319:209–227. [PubMed: 12051947]
- Hilty C, Fernandez C, Wider G, Wuthrich K. Side chain NMR assignments in the membrane protein OmpX reconstituted in DHPC micelles. *J Biomol NMR.* 2002; 23:289–301. [PubMed: 12398349]
- Hilty C, Wider G, Fernandez C, Wuthrich K. Stereospecific assignments of the isopropyl methyl groups of the membrane protein OmpX in DHPC micelles. *J Biomol NMR.* 2003; 27:377–382. [PubMed: 14512734]
- Hyberts SG, Milbradt AG, Wagner AB, Arthanari H, Wagner G. Application of iterative soft thresholding for fast reconstruction of NMR data non-uniformly sampled with multidimensional Poisson Gap scheduling. *J Biomol NMR.* 2012; 52:315–327. [PubMed: 22331404]
- Hyberts SG, Takeuchi K, Wagner G. Poisson-gap sampling and forward maximum entropy reconstruction for enhancing the resolution and sensitivity of protein NMR data. *J Am Chem Soc.* 2010; 132:2145–2147. [PubMed: 20121194]
- Krieger M, Brown MS, Faust JR, Goldstein JL. Replacement of endogenous cholesteryl esters of low density lipoprotein with exogenous cholesteryl linoleate. Reconstitution of a biologically active lipoprotein particle. *J Biol Chem.* 1978; 253:4093–4101. [PubMed: 207690]
- Laskowski RA, Rullmann JA, MacArthur MW, Kaptein R, Thornton JM. AQUA and PROCHECK-NMR: programs for checking the quality of protein structures solved by NMR. *J Biomol NMR.* 1996; 8:477–486. [PubMed: 9008363]

- Linge JP, Habeck M, Rieping W, Nilges M. ARIA: automated NOE assignment and NMR structure calculation. *Bioinformatics*. 2003; 19:315–316. [PubMed: 12538267]
- Lomize MA, Lomize AL, Pogozheva ID, Mosberg HI. OPM: orientations of proteins in membranes database. *Bioinformatics*. 2006; 22:623–625. [PubMed: 16397007]
- MacKerell, ADJ. Atomistic Models and Force Fields. In: Becker, OM.; MacKerell, ADJ.; Roux, B.; Watanabe, M., editors. *Computational Biochemistry and Biophysics*. New York: Marcel Dekker, Inc; 2001. p. 7-38.
- Mazhab-Jafari MT, et al. Membrane-dependent modulation of the mTOR activator Rheb: NMR observations of a GTPase tethered to a lipid-bilayer nanodisc. *J Am Chem Soc*. 2013; 135:3367–3370. [PubMed: 23409921]
- Nath A, Atkins WM, Sligar SG. Applications of phospholipid bilayer nanodiscs in the study of membranes and membrane proteins. *Biochemistry*. 2007; 46:2059–2069. [PubMed: 17263563]
- Plevin MJ, Hamelin O, Boisbouvier J, Gans P. A simple biosynthetic method for stereospecific resonance assignment of prochiral methyl groups in proteins. *J Biomol NMR*. 2011; 49:61–67. [PubMed: 21286785]
- Raschle T, Hiller S, Yu TY, Rice AJ, Walz T, Wagner G. Structural and functional characterization of the integral membrane protein VDAC-1 in lipid bilayer nanodiscs. *J Am Chem Soc*. 2009; 131:17777–17779. [PubMed: 19916553]
- Schwieters CD, Kuszewski JJ, Tjandra N, Clore GM. The Xplor-NIH NMR molecular structure determination package. *J Magn Reson*. 2003; 160:65–73. [PubMed: 12565051]
- Shen Y, Delaglio F, Cornilescu G, Bax A. TALOS+: a hybrid method for predicting protein backbone torsion angles from NMR chemical shifts. *J Biomol NMR*. 2009; 44:213–223. [PubMed: 19548092]
- Shenkarev ZO, et al. Lipid-protein nanodiscs as reference medium in detergent screening for high-resolution NMR studies of integral membrane proteins. *J Am Chem Soc*. 2010; 132:5628–5629. [PubMed: 20356311]
- Susac L, Horst R, Wuthrich K. Solution-NMR characterization of outer-membrane protein A from *E. coli* in lipid bilayer nanodiscs and detergent micelles. *Chembiochem*. 2014; 15:995–1000. [PubMed: 24692152]
- Tugarinov V, Choy WY, Orekhov VY, Kay LE. Solution NMR-derived global fold of a monomeric 82-kDa enzyme. *Proc Natl Acad Sci U S A*. 2005; 102:622–627. [PubMed: 15637152]
- Tugarinov V, Kanelis V, Kay LE. Isotope labeling strategies for the study of high-molecular-weight proteins by solution NMR spectroscopy. *Nat Protoc*. 2006; 1:749–754. [PubMed: 17406304]
- Venditti V, Fawzi NL, Clore GM. Automated sequence- and stereo-specific assignment of methyl-labeled proteins by paramagnetic relaxation and methyl-methyl nuclear Overhauser enhancement spectroscopy. *J Biomol NMR*. 2011; 51:319–328. [PubMed: 21935714]
- Vogt J, Schulz GE. The structure of the outer membrane protein OmpX from *Escherichia coli* reveals possible mechanisms of virulence. *Structure*. 1999; 7:1301–1309. [PubMed: 10545325]
- Xu Y, et al. Automated assignment in selectively methyl-labeled proteins. *J Am Chem Soc*. 2009; 131:9480–9481. [PubMed: 19534551]
- Yu TY, Raschle T, Hiller S, Wagner G. Solution NMR spectroscopic characterization of human VDAC-2 in detergent micelles and lipid bilayer nanodiscs. *Biochim Biophys Acta*. 2012; 1818:1562–1569. [PubMed: 22119777]
- Zhu L, Dyson HJ, Wright PE. A NOESY-HSQC simulation program, SPIRIT. *J Biomol NMR*. 1998; 11:17–29. [PubMed: 9566311]
- Zweckstetter M. NMR: prediction of molecular alignment from structure using the PALES software. *Nat Protoc*. 2008; 3:679–690. [PubMed: 18388951]

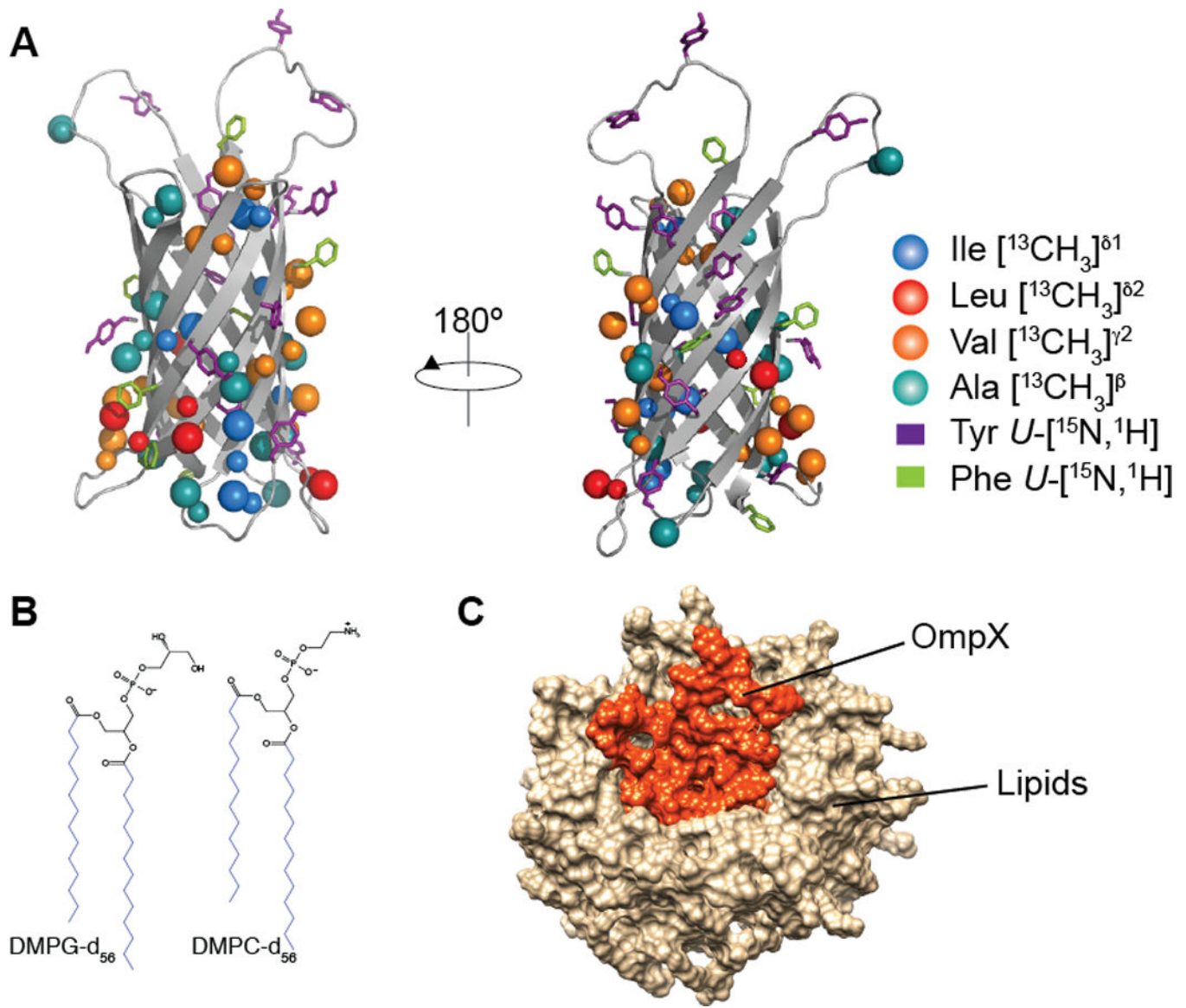


**Figure 1. Amino acid side chain labeling scheme for OmpX in phospholipid nanodiscs**

A) For NMR experiments we used *U*-[ $^2\text{H}$ ,  $^{15}\text{N}$ ]-OmpX that was additionally labeled with *U*-[ $^1\text{H}$ ,  $^{15}\text{N}$ ]-Phe and Tyr and stereospecifically methyl labeled at Ile, Leu, Val and Ala side chains as indicated in the figure. B) For nanodisc preparation, deuterated lipids (DMPC- $d_{56}$ :DMPG- $d_{56}$ =3:1) and our truncated membrane scaffold protein MSP1D1 H5 were used. Lipid head groups were protonated (black), whereas the fatty acids were deuterated (blue). C) Phospholipid nanodisc particle consisting of isotopically labeled OmpX (orange), deuterated lipids (beige) and two copies of the MSP (not shown) surrounding the hydrophobic edge of the bilayer.

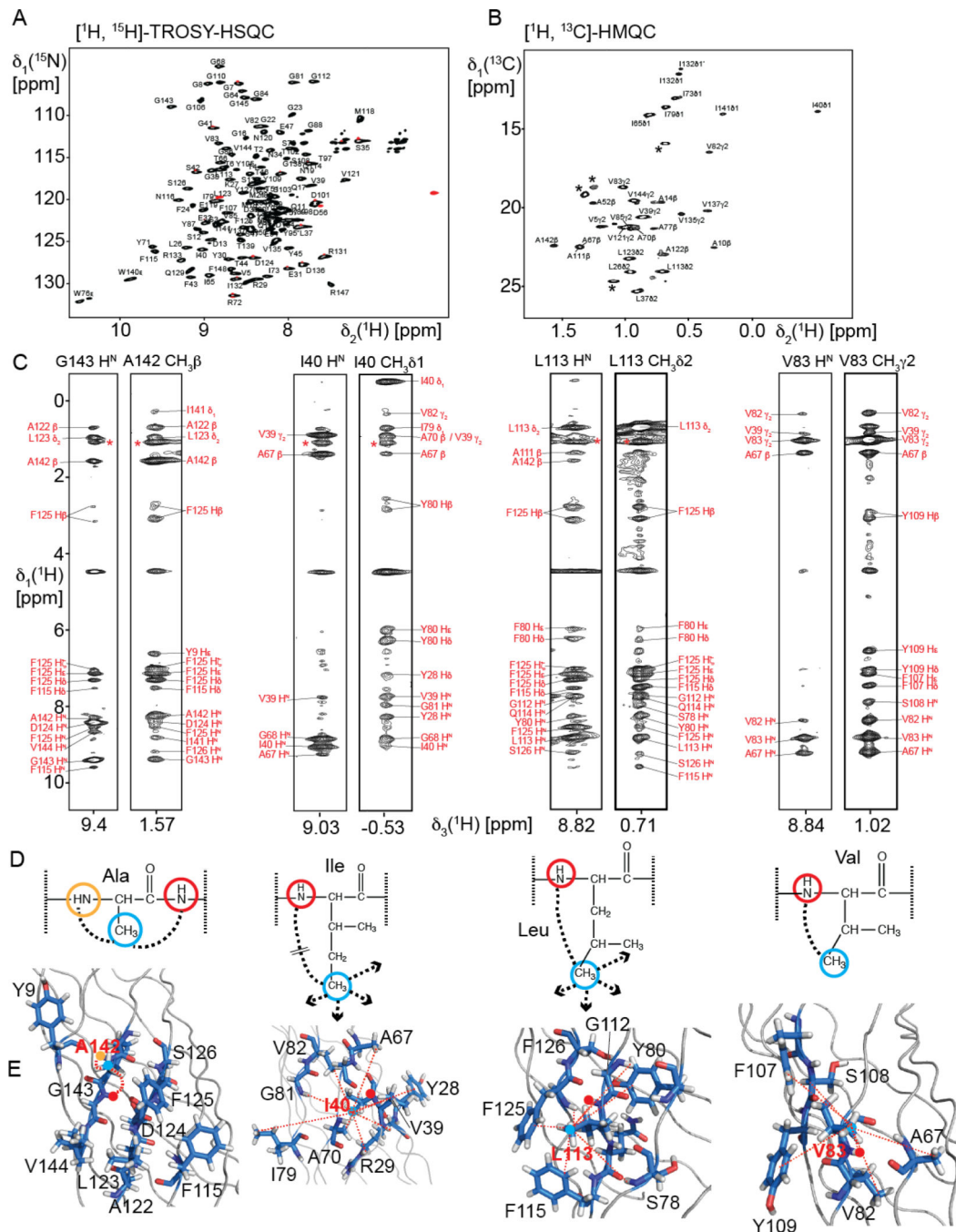


**Figure 2.** NOE-based assignment of methyl side chains of selectively-labeled OmpX in nanodiscs. A) 2D- $[\text{H}, ^{15}\text{N}]$ -TROSY and B) 2D- $[\text{H}, ^{13}\text{C}]$ -HMQC of ILVAFY-labeled OmpX in nanodiscs. Assignments are labeled. Asterisks in B) indicate resonances arising from residual protonation of the fatty acid chains of the lipids. C) Strips of  $^{15}\text{N}$ - and  $^{13}\text{C}$ -edited 3D NOESY experiments of selected Ala, Ile, Leu and Val residues in the protein. The assigned NOE contacts are labeled in red. D) Assignment strategy based on NOE connectivities: backbone amides are labeled in red or orange, methyl groups in blue. Dashed lines indicate expected NOE contact that can be used to establish methyl group assignments.

Due to the use of  $^{14}\text{N}$ -Ala, the amide group of the succeeding residue (red) was used to assign Ala methyl groups. The assignments of Val can be established by a strong NOE between the amide group and the  $\gamma_2$  methyl. For Ile and Leu, due to the large distance between backbone amide and  $\delta$  methyl, long-range tertiary contacts have to be utilized for assignment. E) Structure of OmpX where the observed NOE contacts are shown as red dashed lines. These NOE networks were used for the final assignment of methyl and aromatic resonances.

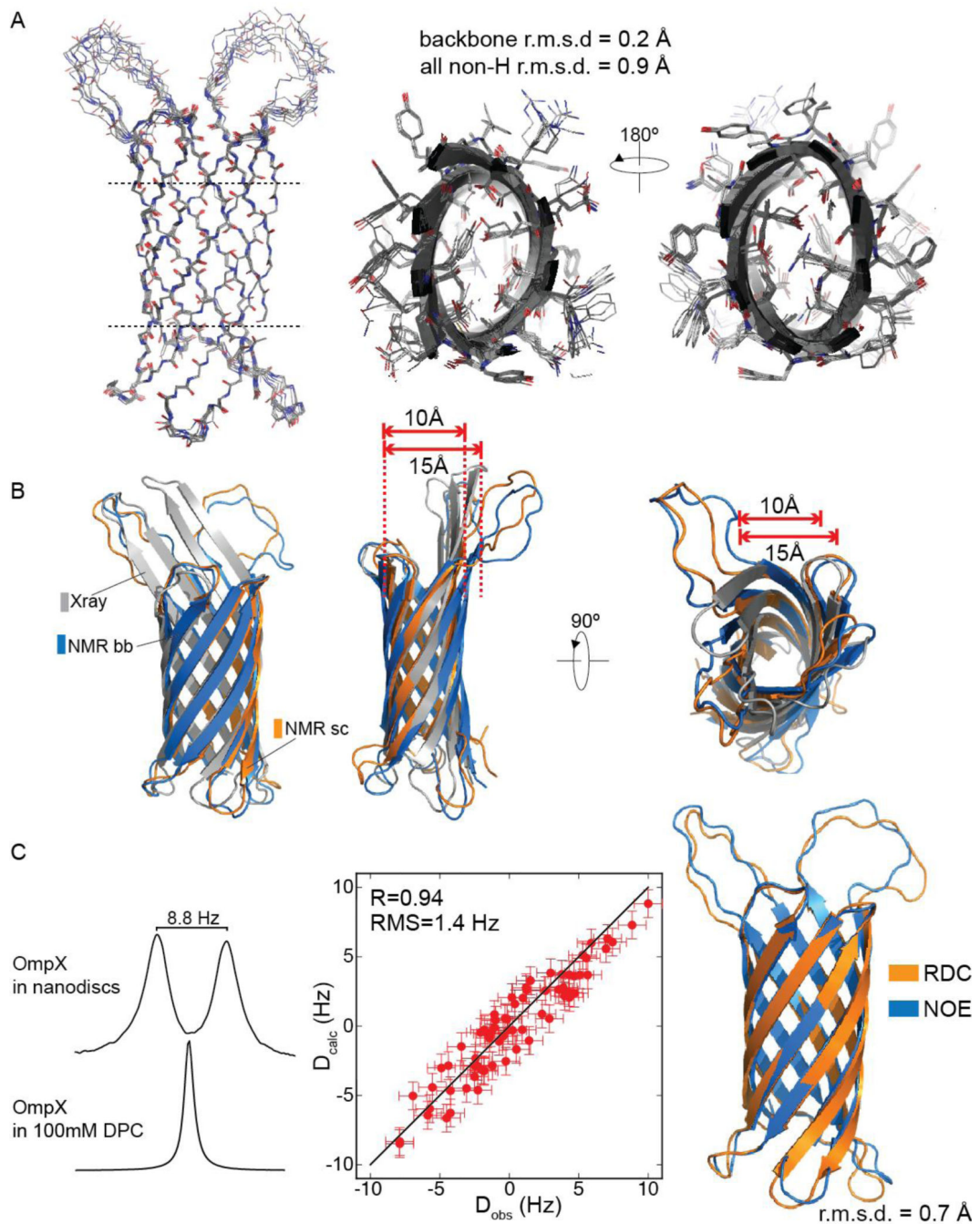


**Figure 3. NMR structure of AILVFI-labeled OmpX in MSP1D1 H5 nanodiscs**

A) 10 lowest-energy structural models have an r.m.s.d. of 0.2 Å for backbone and 0.9 Å for all non-hydrogen atoms within secondary structure elements. Protein side-chain orientation is fairly well defined and almost identical to the crystal structure, especially for side chains oriented towards the interior of the  $\beta$ -barrel. B) Comparison of NOE-based OmpX NMR structures where backbone-only (blue; pdb code: 2M06) or backbone and side-chain restraints (orange) were used vs. the crystal structure (grey; pdb code: 1QJ8). The NOE-based structure of side-chain labeled OmpX shows a narrower  $\beta$ -barrel as compared to the



backbone-NOE structure, similar to the crystal structure. C) H-N Residual dipolar couplings (RDCs) of OmpX in nanodiscs in presence of 10mg/mL Pf1 phage medium at 310K. Phage induced alignment was not possible in the presence of the detergent dodecylphosphocholine (DPC). These RDCs were used for structural refinement of the NOE-based structure, which yielded a good correlation between experimental and back-calculated RDCs. Error bars indicate the experimental error and the errors used for RDC back-calculation, respectively. The structures of OmpX before and after RDC refinement were very similar with a backbone r.m.s.d. of 0.7Å within ordered secondary structure elements.

Author Manuscript

Author Manuscript

Author Manuscript

Author Manuscript

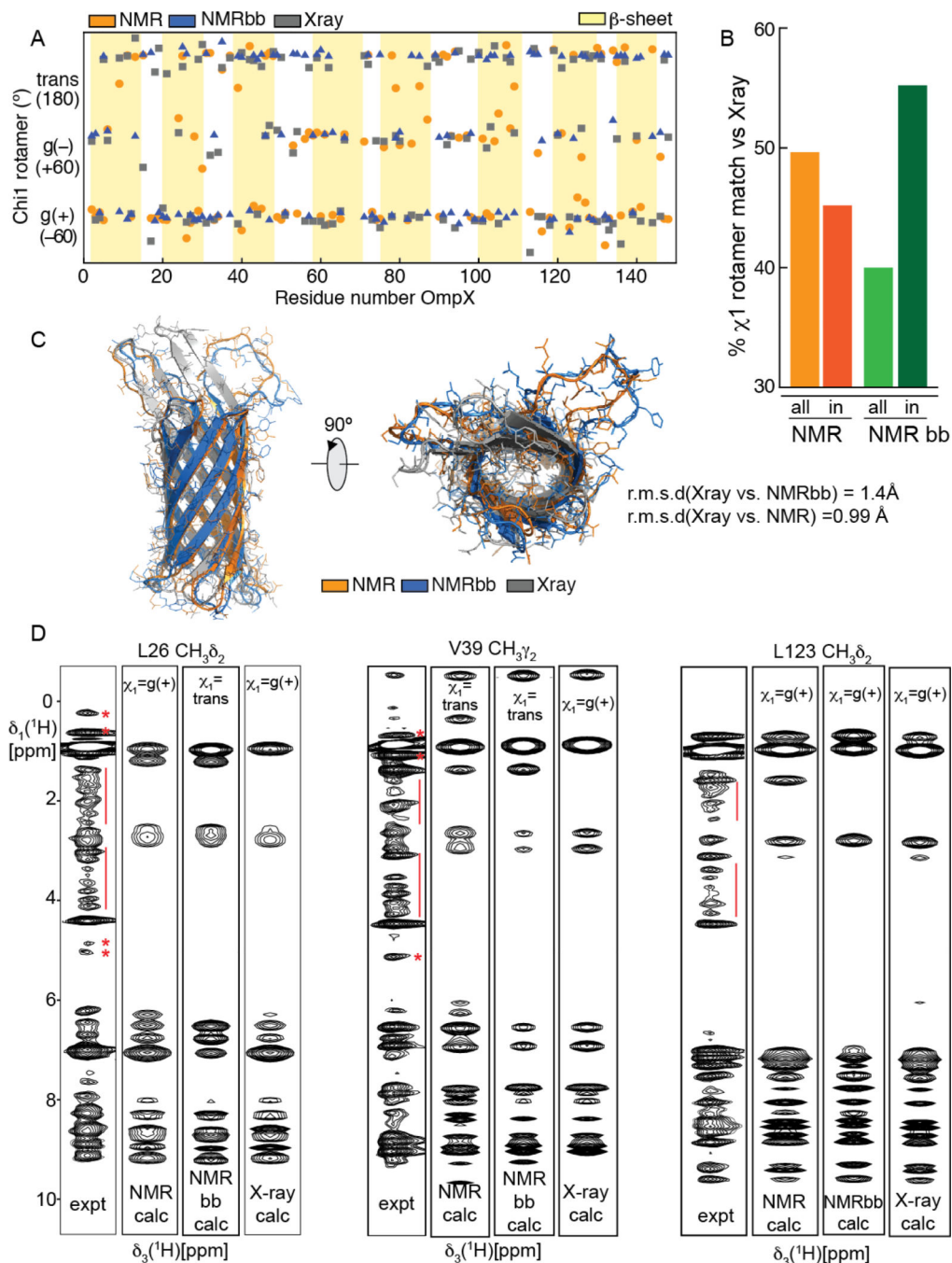


**Figure 4. Validation of NMR structures with NOESY back-calculation**

A) Plot of side chain  $\chi_1$ -rotamer of OmpX structures with the three most favored angles labeled.  $\beta$ -sheets are indicated by yellow boxes. B) Comparison of  $\chi_1$ -rotamers of OmpX structures determined experimentally with NMR including side/chain information (orange) or backbone contacts (green) with the crystal structure (pdb code: 1QJ8). In both NMR structures, the match with the X-ray structure increases for residues pointing inside the  $\beta$ -barrel that are more restricted by packing and NOEs between side-chains. C) Overlay of the three structures show a very low backbone r.m.s.d. but significant differences in the

orientation of the side-chains, especially those pointing toward the lipid bilayer. D) NOESY back-calculation with the program NMRSpiritC++ (in-house modified based on (Zhu et al. 1998)) was used to assess the quality of the obtained structures by comparison with the experimental NOESY spectra. For L26- $\delta$ 2, X-ray and NMR side-chain structures have the same  $\chi$ 1-rotamer and consequently their back-calculated spectra show a better match with the experimental one than the NMR backbone structure. For V39- $\gamma$ 2, back-calculated NOESY strips of both NMR structures fit better than the one back-calculated using the X-ray structure. For L123- $\delta$ 2, all three structures fit very well due to their almost identical  $\chi$ 1-rotamer. In general, this procedure might be a good choice for the refinement of the side-chain orientation of membrane proteins without the need for an explicit structure determination. Red asterisks and bars indicate resonances originating from the residual protonation of the deuterated lipid aliphatic chains and their protonated head groups.

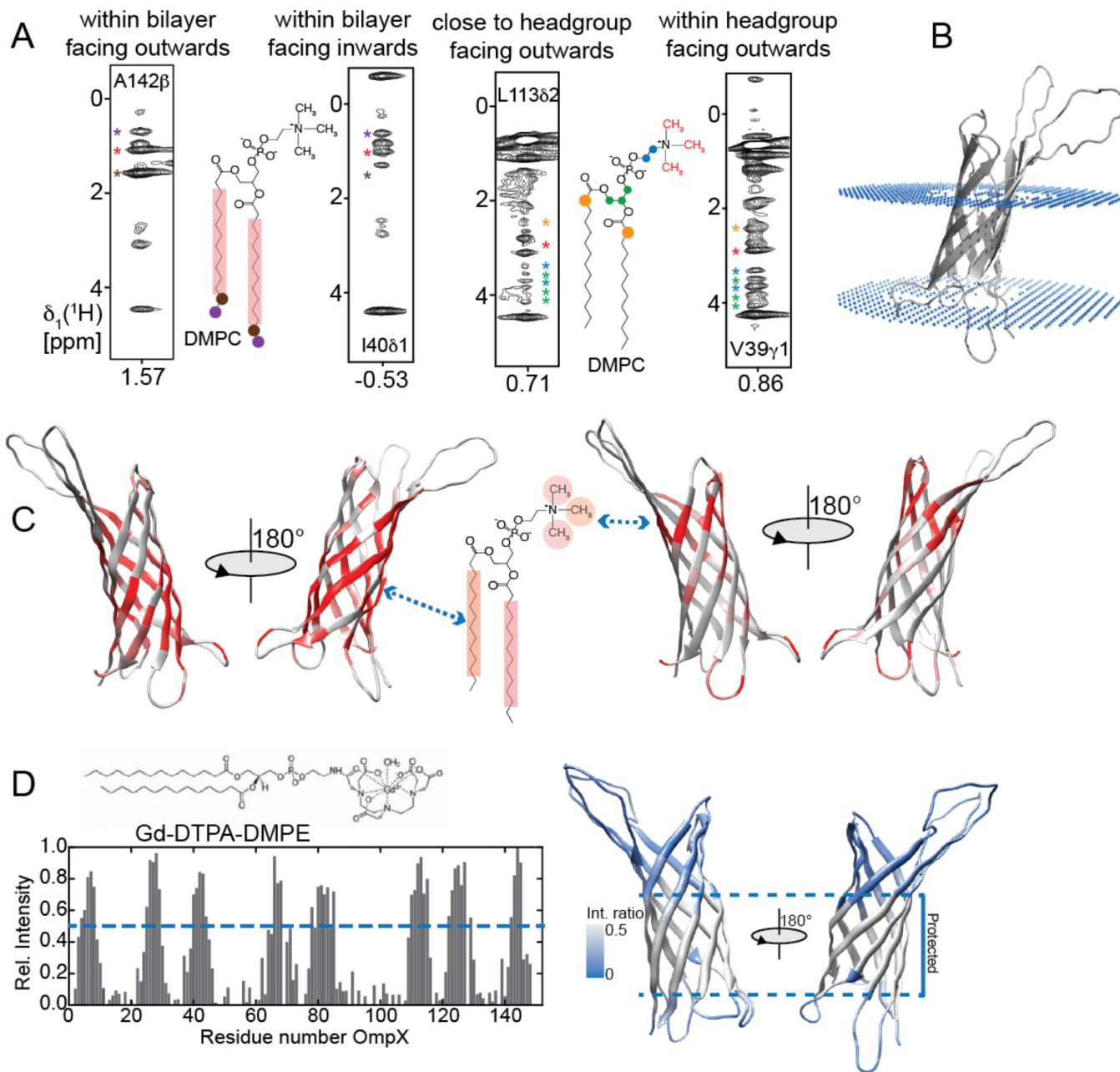


**Figure 5. Determination of the membrane position of OmpX in a lipid bilayer by lipid-protein NOEs and PREs**

A) NOESY strips of OmpX residues at various locations as indicated by the asterisks in the spectra and the circles and shadings on the lipid structures (left panel indicating the fatty acid part of the lipid - red: aliphatic methylene groups; brown:  $\text{C}^{13}$   $\text{CH}_2$  moiety; purple: methyl group; right panel indication the head group region - red: choline moiety; blue: methylene groups adjacent to phosphate; green: CH groups of the glycerol; orange:  $\text{C}^2$  methylene group of the fatty acid). The different location of the protein side-chain give rise to a characteristic NOE pattern that correlated well with their position within the protein and in the lipid bilayer. Resonance assignments of the DMPC lipid were taken from (Susac et al.

2014). B) Membrane position as predicted with the PPM server (<http://opm.phar.umich.edu/server.php>, (Lomize et al. 2006)). OmpX adopts a slightly tilted position in respect to the membrane bilayer surface (blue dots). C) Qualitative pattern of NOEs between OmpX backbone amides and methyl side-chains to the fatty acid or the choline resonances of the lipids. Residues within the  $\beta$ -barrel show strong NOEs to the fatty acid, whereas residues in the head-group region are in close proximity to the choline moiety of DMPC. In addition, this pattern indicates a slight tilt of the  $\beta$ -barrel as predicted by the PPM server. D) OmpX in phospholipid nanodiscs assembled in presence of gadolinium-modified lipids was used to corroborate the NOE patterns shown in C). Residues within the bilayer are not affected by paramagnetic line broadening whereas resonances of residues at the ends of the barrel were markedly weakened or completely disappeared.

**Table 1**

<b>Structural Statistics of OmpX in nanodiscs</b>	
NOEs	587
H-bond restraints	77
Dihedral angles (TALOS) (Shen et al. 2009)	291
Backbone r.m.s.d. in ordered regions <sup>a,c</sup>	0.244±0.051
Heavy atom r.m.s.d. in ordered regions <sup>a,c</sup>	0.878±0.047
<b>Ramachandran Analysis</b>	
Most favored regions (%)	88.5
Additionally allowed (%)	8.2
Generously allowed (%)	1.6
Disallowed (%)	1.6
<b>Deviations from restraints and idealized geometry<sup>c</sup></b>	
Distance restraints (Å)	0.098±0.015
Dihedral angle restraints (°)	0.44±0.014
Bond lengths (Å)	0.0051±0.0008
Angles (°)	1.03±0.01
Impropers (°)	3.09±0.05

<sup>a</sup> Ordered secondary structure elements were used for structural superimposition: 3–14, 20–30, 38–48, 60–71, 78–90, 104–115, 122–132, 135–147; rmsd values are calculated relative to a nonminimized average structure of the ensemble.

<sup>b</sup> Ramachandran analysis with PROCHECK-NMR (Laskowski et al. 1996) was performed on the lowest-energy structure.

<sup>c</sup> Analysis of the 10 lowest-energy structures